Mantle hotspot neon in basalts from the Northwest Lau Back-arc Basin

J. E. Lupton,[1] R. J. Arculus,[2] L. J. Evans,[3] and D. W. Graham[4]

Received 2 February 2012; revised 27 March 2012; accepted 29 March 2012; published 28 April 2012.

[1] The neon isotope compositions of basalts from the Northwest Lau Back-arc Basin reflect three-component mixing between an ocean island basalt (OIB) mantle hotspot component, mid-ocean ridge basalt (MORB) mantle, and atmosphere. Our study confirms that a mantle hotspot signature is present in the neon isotopes of both the Rochambeau Rifts and the Northwest Lau Spreading Center (NWLSC), just as it is in the helium isotopes. Furthermore, the Ne isotope signature in the Rochambeau Rifts lava having the highest $^3He/^4He$ ratio (28 R_a) most closely resembles that observed previously in the highest $^3He/^4He$ lavas from Samoa. The coupled He–Ne isotope systematics are further evidence for incursion into this region of material derived from the Samoan mantle plume. **Citation:** Lupton, J. E., R. J. Arculus, L. J. Evans, and D. W. Graham (2012), Mantle hotspot neon in basalts from the Northwest Lau Back-arc Basin, *Geophys. Res. Lett.*, *39*, L08308, doi:10.1029/2012GL051201.

1. Introduction

[2] The pattern of mantle flow, and the involvement of subducted material plus shallow and deep mantle components in the petrogenesis of basaltic magma in back-arc basins are topics of considerable interest. Isotopic tracers measured in basalts provide some of the most powerful insight to these tectonically complex regions. In this paper we investigate helium and neon isotope variations in lavas from the Northwest Lau Back-arc Basin, which is one of three back-arc extensional zones in the northern Lau Basin (Figure 1).

[3] Lavas from the Northwest Lau Back-arc Basin are known to have anomalous helium isotope ratios compared to what is expected for volcanic rocks that are derived from Earth's upper mantle, such as mid-ocean ridge basalts (MORBs). *Poreda and Craig* [1992] measured elevated $^3He/^4He$ in 3 samples from the Rochambeau Rifts (RR) (up to 22 R_a), providing an early indication of the presence of a hotspot component in this region (see Figure 1). In a more extensive study, *Lupton et al.* [2009] showed that a suite of 29 basalts dredged along the RR and Northwest Lau Spreading Center (NWLSC) all had elevated $^3He/^4He$ (11 to 28 R_a), much higher than the ratio of 7 to 9 R_a typically observed in MORBs. The hotspot helium signature is not confined to the RR, but is also present along the NWLSC extending southward to the Peggy Ridge (PR) (Figure 1). Surprisingly, this hotspot signature appears to be confined to the Northwest Lau Back-arc Basin because samples collected farther east and south along the Mangatolu Triple Junction (MTJ), Northeast Lau Spreading Center (NELSC), Fonualei Rift and Spreading Center (FRSC), and Central Lau Spreading Center (CLSC) all have MORB-like $^3He/^4He$ ratios or lower [*Poreda and Craig*, 1992; *Honda et al.*, 1993a; *Hilton et al.*, 1993; *Lupton et al.*, 2009]. *Turner and Hawkesworth* [1998] proposed that the elevated $^3He/^4He$ ratios, as well as other geochemical anomalies in the RR–NWLSC area, are due to the presence of material derived from the Samoan hotspot that intruded into the northern Lau Basin through a tear in the Pacific plate [*Natland*, 1980]. The highest $^3He/^4He$ ratio observed in the Northwest Lau Back-arc Basin is 28.2 R_a [*Lupton et al.*, 2009], similar to the highest values reported for Samoan basalts by *Farley et al.* [1992] (up to 24 R_a) and *Jackson et al.* [2007] (up to 33.8 R_a). Although the Samoan hotspot appears to be the ultimate source of the high $^3He/^4He$ signature in the Northwest Lau Back-arc Basin, it is surprising that the $^3He/^4He$ ratios are so consistently elevated along the entire length of the RR–NWLSC. The question remains as to whether the elevated $^3He/^4He$ ratios along the RR–NWLSC are the only unequivocal evidence for material derived from the distal Samoan mantle plume.

[4] Neon isotopes offer the possibility of another view of this problem. *Craig and Lupton* [1976] initially showed that the mantle contains neon with elevated $^{20}Ne/^{22}Ne$ distinct from the atmosphere. Since that time, detailed work by numerous investigators has shown that the mantle is characterized by elevated ratios of both $^{20}Ne/^{22}Ne$ and $^{21}Ne/^{22}Ne$ compared to the atmosphere [e.g., *Sarda et al.*, 1988; *Marty*, 1989; *Honda et al.*, 1991; *Poreda and Farley*, 1992; *Moreira et al.*, 1998; *Dixon et al.*, 2000]. Due to the presence of an atmospheric component, the neon in most terrestrial volcanic rocks is a binary mixture of air neon and a mantle end-member [*Farley and Poreda*, 1993; *Ballentine and Barfod*, 2000]. The elevated $^{20}Ne/^{22}Ne$ in mantle-derived rocks and fluids results from the presence of a primitive neon component in the Earth (e.g., "solar Ne" and/or "Ne B" [*Trieloff et al.*, 2000; *Ballentine et al.*, 2005; *Marty,* 2012]). Terrestrial volcanic rocks also have different $^{20}Ne/^{22}Ne$ versus $^{21}Ne/^{22}Ne$ relationships corresponding to the variable addition of nucleogenic ^{21}Ne. This difference manifests itself as different air-mantle mixing lines in the standard 3-isotope plots of $^{20}Ne/^{22}Ne$ versus $^{21}Ne/^{22}Ne$. Most MORBs fall along a mixing line corresponding to relatively higher $^{21}Ne/^{22}Ne$ resulting in a flatter $^{20}Ne/^{22}Ne$ versus $^{21}Ne/^{22}Ne$ slope, while ocean island basalts (OIBs) have relatively lower $^{21}Ne/^{22}Ne$ resulting in a steeper slope. Furthermore,

[1]Pacific Marine Environmental Laboratory, NOAA, Newport, Oregon, USA.
[2]Research School of Earth Sciences, Australian National University, Canberra, ACT, Australia.
[3]Cooperative Institute of Marine Resources Studies, Oregon State University, Newport, Oregon, USA.
[4]College of Earth, Ocean and Atmospheric Sciences, Oregon State University, Corvallis, Oregon, USA.

Corresponding Author: J. E. Lupton, Pacific Marine Environmental Laboratory, NOAA, 2115 SE OSU Dr., Newport, OR 97365, USA. (john.e.lupton@noaa.gov)

0094-8276/12/2012GL051201

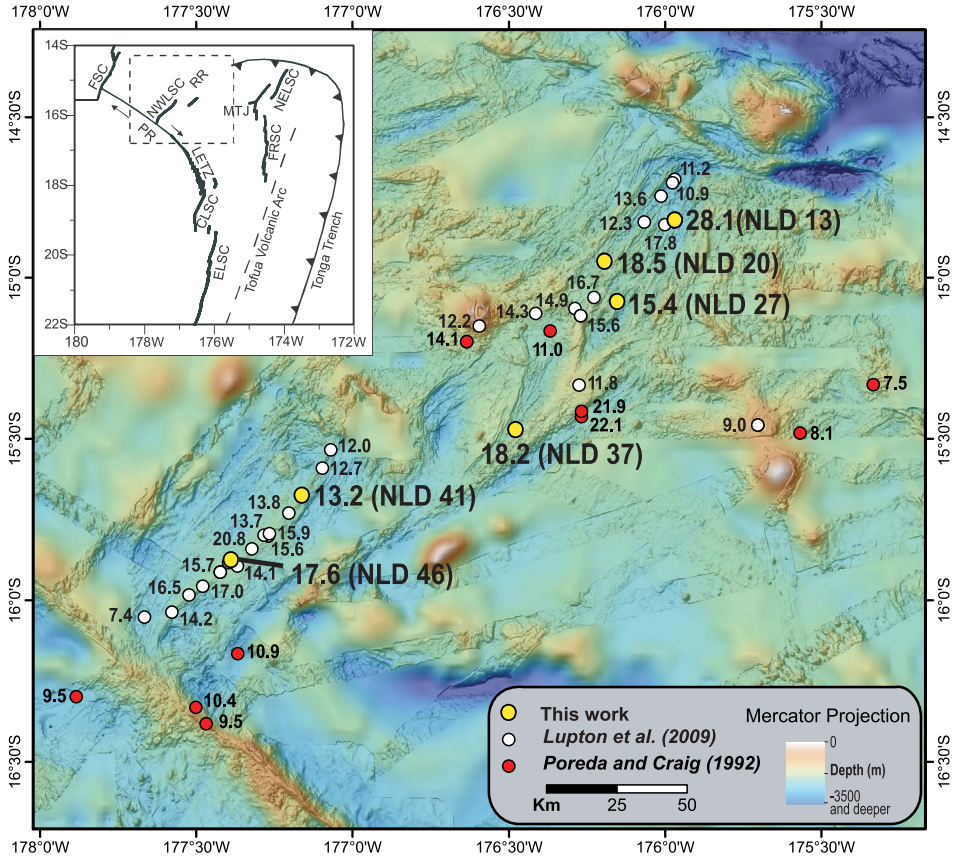

Figure 1. Detailed map showing locations of basalt samples analyzed in this study (yellow circles) along the Northwest Lau Spreading Center (NWLSC) and the Rochambeau Rifts (RR). Results previously reported by *Poreda and Craig* [1992] (red circles) and *Lupton et al.* [2009] (white circles) are also included. Numbers next to the sample locations are helium isotope ratios expressed as R/R_a (where $R = {}^3He/{}^4He$ and $R_a = R_{air} = 1.39 \times 10^{-6}$). The inset shows the plate boundaries and spreading centers in the northern Lau Basin. The dashed box denotes the area covered by the detailed map. FSC = Futuna Spreading Center, NELSC = Northeast Lau Spreading Center, MTJ = Mangatolu Triple Junction (MTJ), FRSC = Fonualei Rift and Spreading Center, PR = Peggy Ridge, LETZ = Lau Extensional Transform Zone, CLSC = Central Lau Spreading Center, ELSC = Eastern Lau Spreading Center. Bathymetry from *Arculus* [2008].

individual ocean island groups appear to have distinct trend lines, implying that their mantle source reservoirs have experienced different amounts of nucleogenic ^{21}Ne addition [e.g., see *Graham*, 2002].

[5] In this paper we present new neon isotopic results for the Northwest Lau Back-arc Basin. For this study we selected six samples from the suite of basalt samples previously analyzed for helium isotopes by *Lupton et al.* [2009]. These samples are designated NLD (Northern Lau Dredge). The results indicate that high $^3He/^4He$ basalts from the RR–NWLSC region have a neon isotope signature that is both distinct from the MORB mantle and consistent with a Samoan mantle plume source.

2. Sampling and Analytical Methods

[6] The samples for this study were dredged from the seafloor during voyage SS07/2008 of the Australian Marine National Facility ship *R/V Southern Surveyor* [*Arculus*, 2008]. Forty-two of these samples were previously analyzed for helium isotopes, 15 from the RR, 14 from the NWLSC, 3 from the PR and LETZ, 9 from the CLSC, and 1 from an off-axis volcano on a bathymetric high northwest of Niua'fo'ou [*Lupton et al.*, 2009]. For the present study, we selected 6 basalt glass samples from this suite for detailed neon isotope analysis, 4 from the RR (NLD-13, -20, -27, and -37) and 2 from the NWLSC (NLD-41 and -46). In order to find gas-rich samples for the neon work, we selected samples that had previously yielded high He concentrations. The map in Figure 1 shows our previously published helium isotope results for samples from the Northwest Lau Back-arc Basin with the six samples for the present study highlighted. For purposes of comparison we also analyzed two MORB glasses from the Juan de Fuca Ridge (JdFR; TT152-21 and TT152-37) previously analyzed for helium isotopes by *Lupton et al.* [1993]. A complete description of our analytical methods is given in the auxiliary material.[1]

3. Results

3.1. Neon Isotopes

[7] Figure 2 shows our neon results presented in the standard 3-isotope plot of $^{20}Ne/^{22}Ne$ versus $^{21}Ne/^{22}Ne$. Data points for atmospheric ($^{20}Ne/^{22}Ne = 9.8$, $^{21}Ne/^{22}Ne = .029$)

[1]Auxiliary materials are available in the HTML. doi:10.1029/2012GL051201.

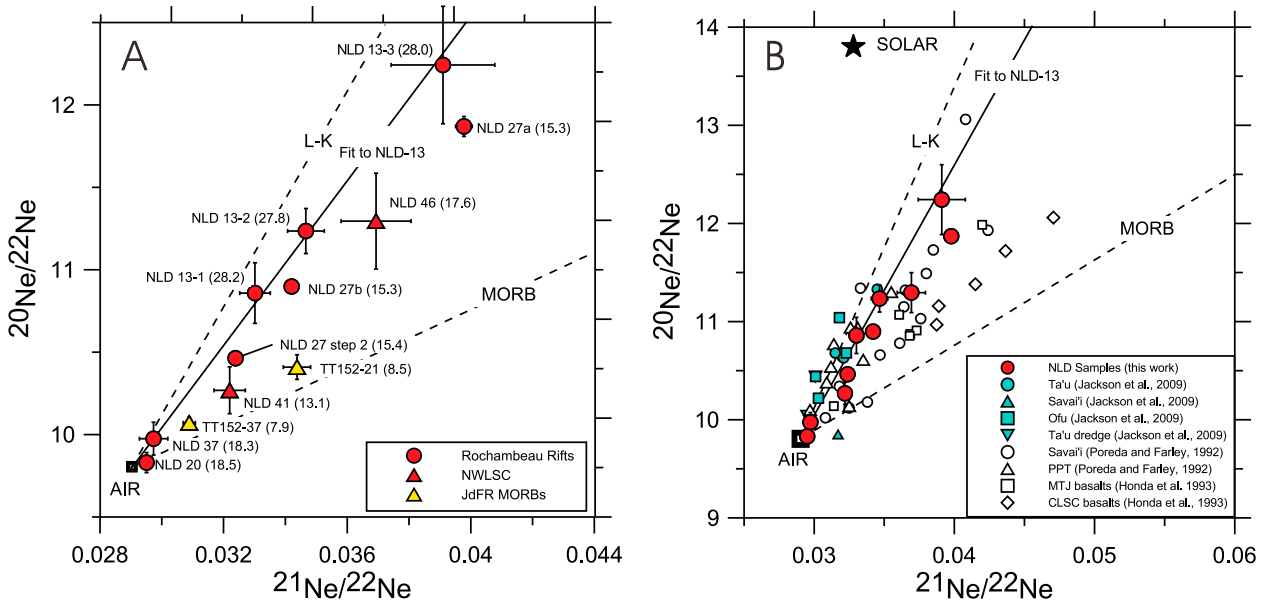

Figure 2. Three-isotope plots of $^{20}Ne/^{22}Ne$ vs. $^{21}Ne/^{22}Ne$. (a) New results include the RR (red circles), the NWLSC (red triangles) and two JdFR basalts (yellow triangles). Error bars are 1-sigma. Numbers in parentheses are $^{3}He/^{4}He$ ratio as R/R_a, where $R = {}^{3}He/^{4}He$ and $R_a = R_{air} = 1.39 \times 10^{-6}$. Solid line is a linear regression fit to 3 analyses of the highest $^{3}He/^{4}He$ sample, NLD-13, and is forced through the air value. Dashed lines show the MORB trend [*Sarda et al.*, 1988; *Moreira et al.*, 1998] and the trend for Loihi-Kilauea [*Honda et al.*, 1991, 1993b; *Hiyagon et al.*, 1992; *Valbracht et al.*, 1997]. (b) Expanded plot that includes results for phenocrysts [*Jackson et al.*, 2009] and ultramafic xenoliths [*Poreda and Farley*, 1992] from Samoan islands and seamounts. Results for other spreading centers in the Lau Basin (MTJ and CLSC) are shown for comparison [*Honda et al.*, 1993a]. Solid and dashed lines are the same as in Figure 2a.

and solar ($^{20}Ne/^{22}Ne = 13.8$, $^{21}Ne/^{22}Ne = .0328$) compositions are shown for comparison. For illustrative purposes, we have also included the trend line for Loihi-Kilauea (L-K) and for MORBs (popping rock) [*Sarda et al.*, 1988; *Honda et al.*, 1991, 1993b; *Hiyagon et al.*, 1992; *Valbracht et al.*, 1997; *Moreira et al.*, 1998]. A complete listing of our helium and neon results is given in Table S1 in the auxiliary material.

[8] Figure 2a shows clearly that basalts from the Northwest Lau Back-arc Basin possess a mantle neon component characterized by excesses in both $^{20}Ne/^{22}Ne$ and $^{21}Ne/^{22}Ne$. One of our sample runs, NLD-13-3, had $^{20}Ne/^{22}Ne$ of 12.24, reflecting a high proportion of mantle neon. Our results plot roughly along a trend indicating binary mixing between a mantle end-member and air. The solid line in Figure 2 is a linear regression fit to our three measurements of NLD-13, the sample with the highest $^{3}He/^{4}He$ ratio (28 R_a). In detail, given our current understanding of noble gases in the Earth [*Marty*, 2012], it is likely that the other samples lie along slightly different trend lines that are not fully resolvable with the present data set (see further discussion below). The slope of the NLD-13 trend corresponds to $^{21}Ne/^{22}Ne_E \sim 0.044$, where $^{21}Ne/^{22}Ne_E$ is the $^{21}Ne/^{22}Ne$ value when $^{20}Ne/^{22}Ne$ is extrapolated to the solar ratio of 13.8. Thus the trend for the Northwest Lau data, while not as steep as that for L-K, is clearly distinct from the MORB trend, falling midway between the trends previously characterized for the Réunion [*Hanyu et al.*, 2001] and Kerguelen [*Valbracht et al.*, 1996] hotspots.

[9] Our new results show unambiguously that a mantle hotspot component (OIB-type Ne) is present in basalts erupted in the Northwest Lau Back-arc Basin. Because this component is also present in the two samples analyzed from the NWLSC (NLD-41 and-46), it indicates that the hotspot signal extends farther south than the Rochambeau Rifts. The presence of this hotspot neon is fully consistent with the high $^{3}He/^{4}He$ ratios measured in the same samples by *Lupton et al.* [2009].

[10] For comparison with the basalts from the Northwest Lau Back-arc Basin, we also analyzed neon in two MORB glasses from the JdFR that had been previously analyzed for helium isotopes by *Lupton et al.* [1993]. Sample TT152-21 had clear enrichments in both $^{20}Ne/^{22}Ne$ and $^{21}Ne/^{22}Ne$ with $^{20}Ne/^{22}Ne$ of 10.41, indicating the presence of clearly resolvable mantle neon. As shown in Figure 2a, these two Juan de Fuca samples define a trend that is distinct from our Lau Basin samples. Notably, both of them overlap the accepted MORB trend line when 2-sigma error bars are considered.

[11] The presence of elevated $^{3}He/^{4}He$ ratios in the volcanic rocks of the Northwest Lau Back-arc Basin has been attributed to intrusion of Samoan hotspot material into the northern Lau Basin [*Poreda and Craig,* 1992; *Turner and Hawkesworth*, 1998; *Lupton et al.*, 2009]. However, a question remains whether this is due to the Samoan plume or to some other, previously unrecognized, hotspot. Because there are only two stable helium isotopes, helium alone cannot unambiguously differentiate between various OIB signatures. However, the three stable isotopes of neon, when combined with helium isotope measurements, offer an additional test. In Figure 2b we compare our neon isotope results for the RR–NWLSC with published neon results for samples from the Samoan Islands and from other sites in the Lau Basin. *Poreda and Farley* [1992] measured helium,

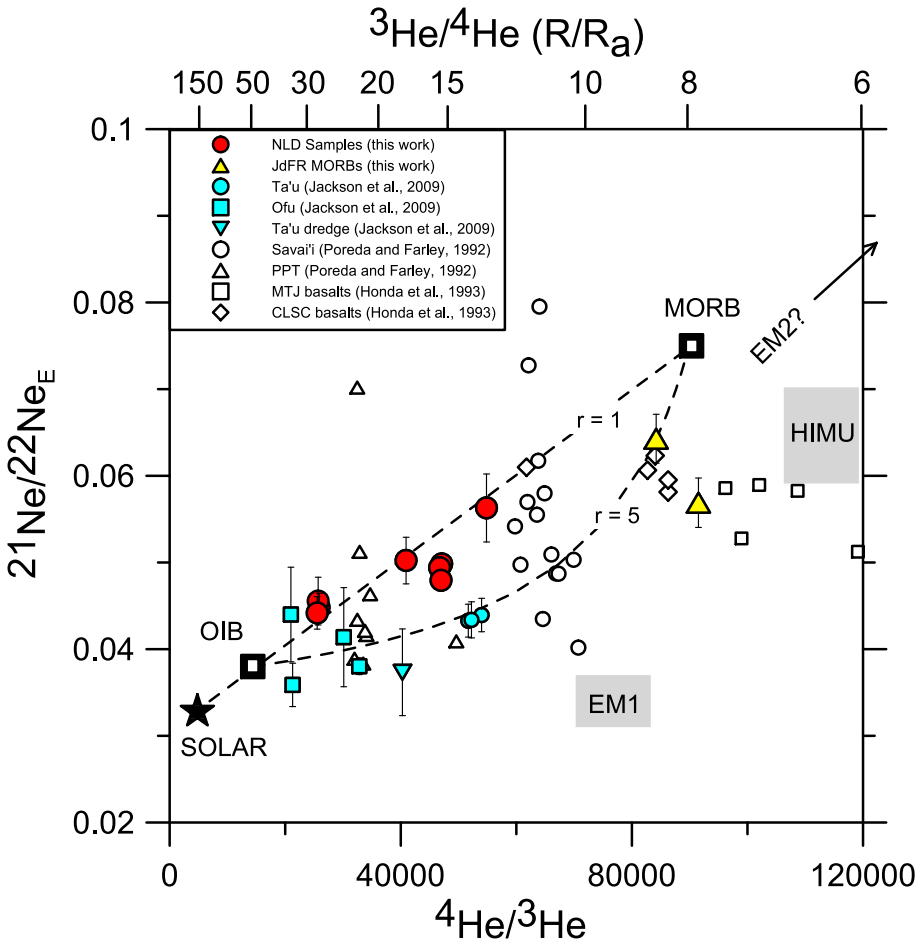

Figure 3. Plot of $^{21}Ne/^{22}Ne_E$ vs. $^{4}He/^{3}He$ for the RR–NWLSC (red circles) and JdFR (yellow triangles), and the Samoan islands [*Poreda and Farley*, 1992; *Jackson et al.*, 2009] and for Lau Basin back-arc spreading centers [*Honda et al.*, 1993a]. Symbols as in Figure 2b. $^{21}Ne/^{22}Ne_E$ was determined by extrapolating the $^{21}Ne/^{22}Ne$ for each sample to the solar $^{20}Ne/^{22}Ne$ ratio of 13.8 using $^{21}Ne/^{22}Ne_E = [0.029 + (^{21}Ne/^{22}Ne - 0.029)/f_{22}]$, where $f_{22} = (^{20}Ne/^{22}Ne - 9.8)/4$ [*Graham*, 2002]. Errors for our data and for those of *Jackson et al.* [2009] were estimated by dividing the 1 sigma $^{21}Ne/^{22}Ne$ error by f_{22}. Results for NLD-20 and -37 were excluded because they did not differ significantly from the atmospheric value. Data points for solar ($^{3}He/^{4}He$ = 150 R_a, $^{21}Ne/^{22}Ne_E$ = .0328), MORB (8 R_a, .0750), and a hotspot or OIB end-member (50 R_a, .038) [*Stuart et al.*, 2003] are shown. Proposed end-member values for several mantle components are also shown for illustration purposes from *Jackson et al.* [2009]; EM1 (9.3 R_a, .034), HIMU (6.3 R_a, .065), and EM2 . Two hypothetical MORB–OIB mixing curves are shown for values of r = 1 and r = 5, where $r = (^{3}He/^{22}Ne)_{MORB}/(^{3}He/^{22}Ne)_{OIB}$.

neon, argon, and xenon isotopes in ultramafic xenoliths from a subaerial site on Savai'i Island, and in samples dredged from Papatua (PPT) seamount. Although there is considerable scatter in their results, in general, their neon results are consistent with our NLD trend (Figure 2b). While noble gas measurements made on Samoan xenoliths clearly reveal the presence of fluids derived from a mantle source that is distinct from the upper mantle, the isotopic signatures are extremely variable. Fluids trapped within xenoliths may partially equilibrate with their host magma during ascent and eruption, and this may tend to obscure the true provenance of the noble gas signal in such samples. In addition, many Samoan xenoliths have experienced metasomatic enrichment during their residence within the upper mantle, and it seems that several fluid "families" can be present in these xenoliths [*Farley et al.*, 1994; *Burnard et al.*, 1998]. For the purpose of our study, we therefore focus our comparison on the noble gas signatures observed in phenocrysts from Samoan hotspot lavas as reported by *Jackson et al.* [2009].

[12] *Jackson et al.* [2009] measured helium and neon isotopes in magmatic phenocrysts in lavas from the Samoan islands of Ta'u, Savai'i and Ofu. Compared to the *Poreda and Farley* [1992] results, the *Jackson et al.* [2009] neon measurements plot along a much steeper slope that is close to the L-K line (Figure 2b). In particular, their result for the high $^{3}He/^{4}He$ (34 R_a) Ofu lava plots to the left of the L-K line and midway between the steep mixing trends for Iceland and the Galapagos Islands [*Dixon et al.*, 2000; *Moreira et al.*, 2001; *Kurz et al.*, 2009]. *Jackson et al.* [2009] assign an extrapolated $^{21}Ne/^{22}Ne_E$ of 0.038 for Samoa, as defined by the result for their high $^{3}He/^{4}He$ Ofu lavas. At first glance, this value appears to be inconsistent with the trend line defined by our Northwest Lau Back-arc Basin lavas. Indeed, almost none of the *Jackson et al.* [2009] results overlap our NLD results even when the errors are considered (Figure 2b). However, as we discuss later, a different picture emerges when the He and Ne isotope results are considered together.

[13] *Honda et al.* [1993a] measured the entire suite of noble gas isotopes in basaltic glass samples from the MTJ and the CLSC (Figure 2b). With the exception of one 11 R_a sample on the CLSC, all of their samples had helium isotope ratios in the MORB range or below, varying from 5.9 to 8.8 R_a [*Honda et al.*, 1993a]. Their neon results all plot above the MORB line in the $^{20}Ne/^{22}Ne$ versus $^{21}Ne/^{22}Ne$ plot, falling between the L-K trend and the MORB trend; a surprising result considering the MORB-like $^3He/^4He$ ratios in their samples. It appears that neon along the MTJ and CLSC has less nucleogenic ^{21}Ne compared to typical MORBs, although the *Honda et al.* [1993a] data set clearly requires a complex interpretation.

3.2. Helium–Neon Relationships

[14] Given our current understanding of the origin of noble gases in the Earth [e.g., *Marty*, 2012] there is no reason to expect that neon isotopes for our samples from the RR–NWLSC should be described by mixing between a single OIB-type end-member and an atmospheric component. The He and Ne isotopes collectively show that three-component mixing is involved, including a hotspot end-member, the upper mantle (MORB source), and air. As a confirmation of this effect, careful examination of Figure 2a shows that our neon results are systematically related to the measured helium isotope ratio. For example, our results for NLD-13, which had the highest $^3He/^4He$ (28 R_a), have lower nucleogenic ^{21}Ne compared to NLD-41 (13 R_a) which had higher ^{21}Ne. A traditional method for displaying He and Ne isotopic results involves first calculating an extrapolated $^{21}Ne/^{22}Ne_E$ for each individual measurement, and then plotting $^{21}Ne/^{22}Ne_E$ versus $^4He/^3He$ [*Moreira et al.*, 1995]. In a sense, this extrapolation removes the atmospheric component from the results. Since the ingrowth of radiogenic ^4He and nucleogenic ^{21}Ne are coupled, the use of the $^4He/^3He$ ratio in this plot facilitates comparison of mixing and radiogenic/nucleogenic processes, which can then be parameterized in terms of the $^3He/^{22}Ne$ ratio [*Graham*, 2002].

[15] Figure 3 shows our He and Ne isotope data plotted as $^{21}Ne/^{22}Ne_E$ versus $^4He/^3He$. Data from Samoan lavas [*Jackson et al.*, 2009], Samoan xenoliths [*Poreda and Farley*, 1992], and Lau Basin basalts [*Honda et al.*, 1993a] are shown for comparison. Data points for solar ($^3He/^4He$ = 150 R_a, $^{21}Ne/^{22}Ne_E$ = .0328), MORB mantle (8 R_a, .0750), and a hotspot end-member (50 R_a, .038) are also shown [*Stuart et al.*, 2003; *Yokochi and Marty*, 2004]. For simplicity, we have computed the $^{21}Ne/^{22}Ne_E$ values by extrapolating each sample to the solar $^{20}Ne/^{22}Ne$ ratio of 13.8. However, the shallow and deep mantle appear to be systematically different in both $^{20}Ne/^{22}Ne$ (upper mantle 12.5, deep mantle 13.8) and $^{21}Ne/^{22}Ne$ (>0.056 and <0.040, respectively). The primordial Ne isotope composition of the upper mantle strongly resembles the implanted neon component in meteorites (Ne-B), while the deep mantle neon more strongly resembles the solar composition [*Trieloff et al.*, 2000; *Ballentine et al.*, 2001, 2005; *Marty*, 2012]. If one were to extrapolate to the Neon-B $^{20}Ne/^{22}Ne$ ratio of 12.5, the distribution of data in our Figure 3 would be slightly altered but the basic picture that emerges below would not change.

[16] For our NLD samples $^{21}Ne/^{22}Ne_E$ and $^4He/^3He$ are positively correlated (Figure 3). The coupled helium-neon results trend toward a hotspot end-member approaching the solar composition and plot along an approximately linear trend between OIB and MORB end-members, corresponding to r = 1, where $r = (^3He/^{22}Ne)_{MORB}/(^3He/^{22}Ne)_{OIB}$. *Graham* [2002] noted that most OIBs fall somewhere in the field bounded by the r = 1 and r = 10 mixing lines. Our results for JdFR basalts, as well as the *Honda et al.* [1993a] results for Lau Basin basalts, plot at a slightly lower $^{21}Ne/^{22}Ne_E$ than the accepted MORB value (if extrapolated to solar $^{20}Ne/^{22}Ne$). While Samoan xenoliths are somewhat scattered [*Poreda and Farley*, 1992], the results for He and Ne in Samoan lavas [*Jackson et al.*, 2009] fall in a narrow field consistent with the r = 5 mixing line (Figure 3). It is notable that the high $^3He/^4He$ Ofu Island lavas (34 and 22–24 R_a) plot very near our 28 R_a sample NLD-13. This suggests that the RR basalts and the Samoan Islands may have a common hotspot He-Ne end-member. However, basalts from the distant Galapagos Islands and Loihi [*Honda et al.*, 1991, 1993b; *Hiyagon et al.*, 1992; *Valbracht et al.*, 1997; *Kurz et al.*, 2009] also plot very near our RR results. Our other NLD samples fall along a slightly different mixing line (r = 1) compared to the Ta'u Island lavas (r = 5). This could be the result of the NLD basalts being derived from a mixed mantle source (hotspot-upper mantle) in which the upper mantle end-member in the northern Lau Basin has a lower $^3He/^{22}Ne$ compared to upper mantle near the Samoan hotspot. We speculate that different melting histories of the mantle end-members, beneath the spreading ridges in the Northwest Lau basin compared to the Samoan islands, may have led to these different mixing trajectories in the He-Ne diagram (Figure 3). Fractionation of He from Ne during mantle melting has been proposed previously on the basis of comparative He-Ne-Ar elemental variations in Hawaiian and MORB basalt glasses [*Hopp and Trieloff*, 2008].

4. Summary and Conclusions

[17] We report here new measurements of neon isotopes in samples from the Northwest Lau Back-arc Basin. The neon in six basalts from the RR and NWLSC has a clear mantle signature as evidenced by elevated $^{20}Ne/^{22}Ne$ and $^{21}Ne/^{22}Ne$ ratios compared to atmospheric neon. Furthermore, in a plot of $^{20}Ne/^{22}Ne$ versus $^{21}Ne/^{22}Ne$ the results plot along a steep trend that departs from the MORB trend line and indicates a hotspot or OIB-type affinity for the neon. Assuming that primordial Ne in the Earth is solar in composition, the $^{20}Ne/^{22}Ne$ versus $^{21}Ne/^{22}Ne$ slope for our highest $^3He/^4He$ (28 R_a) sample extrapolates to $^{21}Ne/^{22}Ne_E$ of ~0.044, significantly lower than the MORB extrapolated value of .075, and only slightly higher than the L-K value of .039. Thus the RR–NWLSC neon falls between the trends for the Réunion and Kerguelen ocean island hotspots. Our study confirms that a mantle hotspot signature is present in the neon isotopes of both the RR and the NWLSC, just as it is in the helium.

[18] The He-Ne isotope systematics considered collectively further support the idea that the hotspot material is ultimately derived from the distal Samoan hotspot. Our sample with the highest $^3He/^4He$ (28 R_a) plots very close to the high $^3He/^4He$ samples from Ofu Island [*Jackson et al.*, 2009]. However, at higher $^4He/^3He$ ratios (lower R/R_a) the two sample sets diverge, with the NLD samples plotting along the r = 1 mixing curve and the Samoan lavas plotting along r = 5 ($r = (^3He/^{22}Ne)_{MORB}/(^3He/^{22}Ne)_{OIB}$; Figure 3).

This difference could be explained by the RR–NWLSC and Samoan island lavas being diluted with MORB-like components having different $^{3}He/^{22}Ne$ ratios.

[19] **Acknowledgments.** We thank the shore- and ship-based staff and crew of the Australian Marine National Facility for their outstanding support of the SS07/2008 research voyage. We are grateful to the governments of Fiji and Tonga for their permission to conduct scientific research in their waters. Susan Merle helped with the graphics, and Sandra Bigley helped with editing. Pete Burnard and Robert Poreda provided constructive reviews. This work was supported by the NOAA Vents Program and the Marine Geology & Geophysics program of the National Science Foundation. This is PMEL contribution 3821.

[20] The Editor thanks Pete Burnard and Robert J. Poreda for assisting with the evaluation of this paper.

References

Arculus, R. J. (2008), Charter voyage SS07-2008: Structure, evolution, petrology, and hydrothermal activity of spreading centres in the Northern Lau Backarc Basin, annual report, Mar. Natl. Facil., CSIRO Mar. and Atmos. Res., Hobart, Tasmania, Australia. [Available at http://www.marine.csiro.au/nationalfacility/voyagedocs/2008/index.htm.]

Ballentine, C. J., and D. N. Barfod (2000), The origin of air-like noble gases in MORB and OIB, *Earth Planet. Sci. Lett.*, *180*, 39–48, doi:10.1016/S0012-821X(00)00161-8.

Ballentine, C. J., D. Porcelli, and R. Wieler (2001), Noble gases in mantle plumes, *Science*, *291*, 2269, doi:10.1126/science.291.5512.2269a.

Ballentine, C. J., B. Marty, B. S. Lollar, and M. Cassidy (2005), Neon isotopes constrain convection and volatile origin in the Earth's mantle, *Nature*, *433*, 33–38, doi:10.1038/nature03182.

Burnard, P. G., K. A. Farley, and G. Turner (1998), Multiple fluid pulses in a Samoan harzburgite, *Chem. Geol.*, *147*, 99–114, doi:10.1016/S0009-2541(97)00175-7.

Craig, H., and J. E. Lupton (1976), Primordial neon, helium, and hydrogen in oceanic basalts, *Earth Planet. Sci. Lett.*, *31*, 369–385, doi:10.1016/0012-821X(76)90118-7.

Dixon, E. T., M. Honda, I. McDougall, I. H. Campbell, and I. Sigurdsson (2000), Preservation of near-solar neon isotopic ratios in Icelandic basalts, *Earth Planet. Sci. Lett.*, *180*, 309–324, doi:10.1016/S0012-821X(00)00164-3.

Farley, K. A., and R. J. Poreda (1993), Mantle neon and atmospheric contamination, *Earth Planet. Sci. Lett.*, *114*, 325–339, doi:10.1016/0012-821X(93)90034-7.

Farley, K. A., J. H. Natland, and H. Craig (1992), Binary mixing of enriched and undegassed (primitive?) mantle components (He, Sr, Nd, Pb) in Samoan lavas, *Earth Planet. Sci. Lett.*, *111*, 183–199, doi:10.1016/0012-821X(92)90178-X.

Farley, K. A., R. J. Poreda, and T. C. Onstott (1994), Noble gases in deformed xenoliths from an ocean island: Characterization of a metasomatic fluid, in *Noble Gas Geochemistry and Cosmochemistry*, edited by J. Matsuda, pp. 159–178, Terra Sci., Tokyo.

Graham, D. W. (2002), Noble gas isotope geochemistry of mid-ocean ridge and ocean island basalts: Characterization of mantle source reservoirs, in *Noble Gases in Geochemistry and Cosmochemistry*, *Rev. Mineral. Geochem.*, vol. 47, edited by D. Porcelli, R. Wieler, and C. Ballentine, pp. 247–317, Mineral. Soc. Am., Washington, D. C., doi:10.2138/rmg.2002.47.8

Hanyu, T., T. J. Dunai, G. R. Davies, I. Kaneoka, S. Nohda, and K. Uto (2001), Noble gas study of the Reunion hotspot: Evidence for less-degassed mantle sources, *Earth Planet. Sci. Lett.*, *193*, 83–98, doi:10.1016/S0012-821X(01)00489-7.

Hilton, D. R., K. Hammerschmidt, G. Loock, and H. Friedrichsen (1993), Helium and argon isotope systematics of the central Lau Basin and Valu Fa Ridge: Evidence of crust/mantle interactions in a back-arc basin, *Geochim. Cosmochim. Acta*, *57*, 2819–2841, doi:10.1016/0016-7037(93)90392-A.

Hiyagon, H., M. Ozima, B. Marty, S. Zashu, and H. Sakai (1992), Noble gases in submarine glasses from mid-oceanic ridges and Loihi seamount: Constraints on the early history of the Earth, *Geochim. Cosmochim. Acta*, *56*, 1301–1316, doi:10.1016/0016-7037(92)90063-O.

Honda, M., I. McDougall, D. B. Patterson, A. Doulgeris, and D. A. Clague (1991), Possible solar noble-gas component in Hawaiian basalts, *Nature*, *349*, 149–151, doi:10.1038/349149a0.

Honda, M., D. B. Patterson, I. McDougall, and T. J. Falloon (1993a), Noble gases in submarine pillow basalt glasses from the Lau Basin: Detection of a solar component in backarc basin basalts, *Earth Planet. Sci. Lett.*, *120*, 135–148, doi:10.1016/0012-821X(93)90235-2.

Honda, M., I. McDougall, D. B. Patterson, A. Doulgeris, and D. A. Clague (1993b), Noble gases in submarine pillow basalt glasses from Loihi and Kilauea, Hawaii: A solar component in the Earth, *Geochim. Cosmochim. Acta*, *57*, 859–874, doi:10.1016/0016-7037(93)90174-U.

Hopp, J., and M. Trieloff (2008), Helium deficit in high-$^{3}He/^{4}He$ parent magmas: Predegassing fractionation, not a "helium paradox," *Geochem. Geophys. Geosyst.*, *9*, Q03009, doi:10.1029/2007GC001833.

Jackson, M. G., M. D. Kurz, S. R. Hart, and R. K. Workman (2007), New Samoan lavas from Ofu Island reveal a hemispherically heterogeneous high $^{3}He/^{4}He$ mantle, *Earth Planet. Sci. Lett.*, *264*, 360–374, doi:10.1016/j.epsl.2007.09.023.

Jackson, M. G., M. D. Kurz, and S. R. Hart (2009), Helium and neon isotopes in phenocrysts from Samoan lavas: Evidence for heterogeneity in the terrestrial high $^{3}He/^{4}He$ mantle, *Earth Planet. Sci. Lett.*, *287*, 519–528, doi:10.1016/j.epsl.2009.08.039.

Kurz, M. D., J. Curtice, D. Fornari, D. Geist, and M. Moreira (2009), Primitive neon from the center of the Galapagos hotspot, *Earth Planet. Sci. Lett.*, *286*, 23–34, doi:10.1016/j.epsl.2009.06.008.

Lupton, J. E., D. W. Graham, J. R. Delaney, and H. P. Johnson (1993), Helium isotope variations in Juan de Fuca Ridge Basalts, *Geophys. Res. Lett.*, *20*, 1851–1854, doi:10.1029/93GL01271.

Lupton, J. E., R. J. Arculus, R. R. Greene, L. J. Evans, and C. I. Goddard (2009), Helium isotope variations in seafloor basalts from the Northwest Lau Backarc Basin: Mapping the influence of the Samoan hotspot, *Geophys. Res. Lett.*, *36*, L17313, doi:10.1029/2009GL039468.

Marty, B. (1989), Neon and xenon isotopes in MORB: Implications for the Earth-atmosphere evolution, *Earth Planet. Sci. Lett.*, *94*, 45–56, doi:10.1016/0012-821X(89)90082-4.

Marty, B. (2012), The origins and concentrations of water, carbon, nitrogen and noble gases on Earth, *Earth Planet. Sci. Lett.*, *313–314*, 56–66, doi:10.1016/j.epsl.2011.10.040.

Moreira, M., T. Staudacher, P. Sarda, J.-G. Schilling, and C. J. Allègre (1995), A primitive plume neon component in MORB: The Shona ridge anomaly, South Atlantic (51–52°S), *Earth Planet. Sci. Lett.*, *133*, 367–377, doi:10.1016/0012-821X(95)00080-V.

Moreira, M., J. Kunz, and C. Allègre (1998), Rare gas systematics in popping rock: Isotopic and elemental compositions in the upper mantle, *Science*, *279*, 1178–1181, doi:10.1126/science.279.5354.1178.

Moreira, M., C. Gautheron, K. Breddam, J. Curtice, and M. D. Kurz (2001), Solar neon in the Icelandic mantle: New evidence for an undegassed lower mantle, *Earth Planet. Sci. Lett.*, *185*, 15–23, doi:10.1016/S0012-821X(00)00351-4.

Natland, J. (1980), The progression of volcanism in the Samoan linear volcanic chain, *Am. J. Sci.*, *280*, 709–735.

Poreda, R. J., and H. Craig (1992), He and Sr isotopes in the Lau Basin mantle: Depleted and primitive mantle components, *Earth Planet. Sci. Lett.*, *113*, 487–493, doi:10.1016/0012-821X(92)90126-G.

Poreda, R. J., and K. A. Farley (1992), Rare gases in Samoan xenoliths, *Earth Planet. Sci. Lett.*, *113*, 129–144, doi:10.1016/0012-821X(92)90215-H.

Sarda, P., T. Staudacher, and C. J. Allègre (1988), Neon isotopes in submarine basalts, *Earth Planet. Sci. Lett.*, *91*, 73–88, doi:10.1016/0012-821X(88)90152-5.

Stuart, F., S. Lass-Evans, J. D. Fitton, and R. M. Ellam (2003), High $^{3}He/^{4}He$ ratios in picritic basalts from Baffin Island and the role of a mixed reservoir in mantle plumes, *Nature*, *424*, 57–59, doi:10.1038/nature01711.

Trieloff, M., J. Kun, D. A. Clague, D. Harrison, and C. J. Allègre (2000), The nature of pristine noble gases in mantle plumes, *Science*, *288*, 1036–1038, doi:10.1126/science.288.5468.1036.

Turner, S., and C. Hawkesworth (1998), Using geochemistry to map mantle flow beneath the Lau Basin, *Geology*, *26*, 1019–1022, doi:10.1130/0091-7613(1998)026<1019:UGTMMF>2.3.CO;2.

Valbracht, P. J., M. Honda, T. Matsumoto, N. Mattielli, I. McDougall, R. Ragettli, and D. Weis (1996), Helium, neon and argon isotope systematics in Kerguelen ultramafic xenoliths: Implications for mantle source signatures, *Earth Planet. Sci. Lett.*, *138*, 29–38, doi:10.1016/0012-821X(95)00226-3.

Valbracht, P. J., T. J. Staudacher, A. Malahoff, and C. J. Allègre (1997), Noble gas systematics of deep rift zone glasses from Loihi Seamount, Hawaii, *Earth Planet. Sci. Lett.*, *150*, 399–411, doi:10.1016/S0012-821X(97)00094-0.

Yokochi, R., and B. Marty (2004), A determination of the neon isotopic composition of the deep mantle, *Earth Planet. Sci. Lett.*, *225*, 77–88, doi:10.1016/j.epsl.2004.06.010.

Detailed Analytical Methods

Large chips of volcanic glass (~0.8 to 1.2 g) were cleaned with distilled water and acetone, and then loaded into stainless steel crusher tubes. Blanks were run on each of the crusher tubes before each analysis. Gases were released by crushing the samples to ~100 microns size *in vacuo*. Condensible gases (H_2O and CO_2) were removed on a trap at -195°C. The non-condensible fraction was then exposed to a hot Ti getter, followed by exposure to a charcoal finger at -195°C. The remaining gases, mainly He and Ne, were then exposed to a low temperature charcoal "cryotrap" held at ~38°K, which traps 98% of the Ne while leaving the He in the gas phase. Careful tests of this He-Ne separation have confirmed that Ne is quantitatively retained on the cryotrap without significant isotopic fractionation.

The first part of the analysis consisted of admitting the He fraction into the mass spectrometer. Because of the large sample size and the high He/Ne ratio in these samples, the He fraction was divided statically in order to adjust the sample size. Both the He and Ne measurements were made at the Helium Isotope Laboratory, NOAA/PMEL, Newport, Oregon on a 21-cm radius, dual collector, sector-type mass spectrometer specially designed for helium isotope measurements. For the helium measurements the instrument was operated in dual-collector mode. Helium isotope measurements were standardized against samples of marine air and also against our MM (16.5 R_a) geothermal standard gas [*Lupton and Evans*, 2004]. Precision (2-sigma) for the helium isotope determinations is about 0.5% or about 0.05 R_a. The helium blanks averaged 1.3×10^{-10} cc STP He, and were typically less than 0.02% of the sample.

After completion of the He analysis, the cryotrap was raised to ~120°K, releasing the Ne. For the Ne analysis, all of the measurements were made on the electron multiplier collector normally used for detecting the weak ^{3}He beam. Due to the relatively low ~70 ns dead time of the pulse counting electronics, we were able to accommodate collection of all three neon isotopes on this single collector without encountering problems with pulse pile-up. In some cases the ^{20}Ne pulse rate approached 500,000 cts/sec, which required only a 3.7 % correction for missed pulses. Switching between the Ne peaks was implemented by changing the mass spectrometer acceleration voltage with the magnetic field at a constant setting. For the neon analysis, considerable care was taken to minimize the contribution of the inlet system and mass spectrometer blanks. As mentioned above, blanks were run on each of the crusher tubes before each analysis. A trap containing ~5 g charcoal held at -195°C was included in the mass spectrometer static volume for the Ne analyses, which considerably reduced the contribution from doubly-ionized argon and CO_2. The blanks were found to be reproducible within ~ 1.5% (1-sigma) for all three Ne isotopes. Because the blank signal has a slight time dependence, we instituted a time-dependent scheme for carrying out the blank corrections. We subtracted slightly different blank signals at different times in the sample run corresponding to the time evolution of the blank run. This produced more stable ^{20}Ne/^{22}Ne and ^{21}Ne/^{22}Ne ratios during the run as compared with subtracting a single time-independent blank correction. For most of the samples, a single crushing step consisting of ~130 crushing "whacks" was used to release gases. We analyzed our most gas-rich sample NLD-27 three times. On one of these analyses, designated NLD 27-step 2, we first exposed the sample to ~ 5 crusher whacks, pumped these gases away, and then proceeded with the normal extraction procedure. As can be seen in the section which follows, this appeared to reduce the total He and Ne yield without a substantial improvement in the Ne isotope results.

Our Ne isotope results were standardized using small aliquots of marine air. The Ne blanks averaged 4.7×10^{-11} cc STP Ne. The percentage of the sample from the Ne blank ranged from 3% for NLD 27-b up to 50% for NLD-13 and -46. The total uncertainties for the Ne isotope results vary greatly because we have propagated the uncertainties associated with variability in the blanks. For example, for NLD-46 the uncertainty is higher because the sample had only 4.6×10^{-11} cc STP Ne, about equal to the size of the blank.

References

Lupton, J., and L. Evans (2004), The atmospheric helium isotope ratio: Is it changing?, *Geophys. Res. Lett. 31*, L13101, doi:1029/2004GL020041.

Sample	Latitude	Longitude	[He] (ccSTP/g)	[Ne] (ccSTP/g)	3He/4He (R/Ra)	Weight (g)	20Ne/22Ne	1 σ	21Ne/22Ne	1 σ	Reference
Rochambeau Rifts											
NLD 13a	-14.826	-175.971	1.15E-06		28.10	0.36					[1]
NLD 13b	-14.826	-175.971	5.42E-07		28.12	0.48					[1]
NLD 13-1	-14.826	-175.971	9.62E-07	5.54E-11	28.17	0.90	10.859	0.184	0.03302	0.00050	
NLD 13-2	-14.826	-175.971	9.90E-07	4.22E-11	27.78	1.78	11.235	0.137	0.03466	0.00059	
NLD 13-3	-14.826	-175.971	8.70E-07	2.56E-11	28.00	1.73	12.242	0.356	0.03906	0.00168	
NLD 20	-14.944	-176.195	2.35E-06		18.55	0.49					[1]
NLD 20	-14.944	-176.195	1.53E-06	1.88E-10	18.50	0.90	9.830	0.061	0.02951	0.00020	
NLD 27-2	-15.071	-176.153	2.11E-05		15.36	0.11					[1]
NLD 27-a	-15.071	-176.153	1.43E-05	5.28E-10	15.28	0.98	11.870	0.060	0.03978	0.00027	
NLD 27-b	-15.071	-176.153	1.83E-05	1.36E-09	15.32	0.80	10.898	0.040	0.03420	0.00019	
NLD 27 step2	-15.071	-176.153	6.02E-06	6.54E-10	15.40	0.78	10.463	0.029	0.03239	0.00015	
NLD 37	-15.472	-176.481	2.01E-07		18.24	0.44					[1]
NLD 37	-15.472	-176.481	4.69E-08	7.94E-11	18.32	1.00	9.975	0.099	0.02973	0.00046	
Northwest Lau Spreading Center											
NLD 41b	-15.674	-177.161	3.28E-06		13.18	0.68					[1]
NLD 41	-15.674	-177.161	1.17E-06	9.27E-11	13.12	0.99	10.269	0.113	0.03220	0.00046	
NLD 46	-15.886	-177.395	1.65E-06		17.61	0.58					[1]
NLD 46	-15.886	-177.395	1.30E-06	4.69E-11	17.58	0.88	11.295	0.203	0.03693	0.00100	
Juan de Fuca Ridge											
TT152-37[a]	44.618	-130.390	1.73E-06		7.89						[2]
TT152-37	44.618	-130.390	6.75E-06	4.96E-10	7.86	1.24	10.071	0.030	0.03089	0.00019	
TT152-21[b]	46.925	-129.262	1.13E-06		8.54						[2]
TT152-21	46.925	-129.262	6.98E-06	2.75E-10	8.54	0.87	10.409	0.065	0.03437	0.00043	
Average Blank[c]			1.30E-10	4.70E-11			8.848	0.054	0.0262	0.00035	
AIR					1		9.8		0.0290		
MORB					8						
SOLAR					150		13.8		0.0328		

[a]Average of 6 measurements
[b]Average of 2 measurements
[c]Average blank [He] and [Ne] are cc STP
References: [1] Lupton et al. [2009]; [2] Lupton et al. [1993]; all other values this work